

Vinculin Promotes Cell Spreading by Mechanically Coupling Integrins to the Cytoskeleton

ROBERT M. EZZELL,^{*,1} WOLFGANG H. GOLDMANN,^{*} NING WANG,[†]
NATESH PARASHARAMA,^{*} AND DONALD E. INGBER[‡]

^{*}*Surgery Research Laboratories, Massachusetts General Hospital, Department of Surgery, Harvard Medical School, Charlestown, Massachusetts 02129; and* [†]*Physiology Program, Harvard School of Public Health, ‡Departments of Pathology and Surgery, Children's Hospital and Harvard Medical School, Boston, Massachusetts 02115*

Mouse F9 embryonic carcinoma 5.51 cells that lack the cytoskeletal protein vinculin spread poorly on extracellular matrix compared with wild-type F9 cells or two vinculin-transfected clones (5.51Vin3 and Vin4; Samuels *et al.*, 1993, *J. Cell Biol.* 121, 909–921). In the present study, we used this model system to determine how the presence of vinculin promotes cytoskeletal alterations and associated changes in cell shape. Microscopic analysis of cell spreading at early times, revealed that 5.51 cells retained the ability to form filopodia; however, they could not form lamellipodia, assemble stress fibers, or efficiently spread over the culture substrate. Detergent (Triton X-100) studies revealed that these major differences in cell morphology and cytoskeletal organization did not result from differences in levels of total polymerized or cross-linked actin. Biochemical studies showed that 5.51 cells, in addition to lacking vinculin, exhibited slightly reduced levels of α -actinin and paxillin in their detergent-insoluble cytoskeleton. The absence of vinculin correlated with a decrease in the mechanical stiffness of the integrin-cytoskeleton linkage, as measured using cell magnetometry. Furthermore, when vinculin was replaced by transfection in 5.51Vin3 and 5.51Vin4 cells, the levels of cytoskeletal-associated α -actinin and paxillin, the efficiency of transmembrane mechanical coupling, and the formation of actin stress fibers were all restored to near wild-type levels. These findings suggest that vinculin may promote cell spreading by stabilizing focal adhesions and transferring mechanical stresses that drive cytoskeletal remodeling, rather than by altering the total level of actin polymerization or cross-linking. © 1997 Academic Press

INTRODUCTION

One of the links between the actin cytoskeleton and the plasma membrane, the focal adhesion, consists of

¹To whom correspondence and reprint requests should be addressed at Massachusetts General Hospital, Surgery Research Unit, 149 13th Street, Charlestown, MA 02129. Fax: (617) 726-5414. E-mail: ezzell@helix.mgh.harvard.edu.

a complex of proteins that assemble at sites of attachment of the cell to the extracellular matrix [1]. The transmembrane proteins mediating these contacts are members of the integrin family of extracellular matrix (ECM) receptors. Integrins are heterodimeric complexes in which both chains span the plasma membrane bilayer once, and the cytoplasmic domain is responsible for linkage of the actin cytoskeleton. A number of proteins are found in focal adhesions at the intracellular face of the plasma membrane, including vinculin, α -actinin, paxillin, and talin [2, 3]. Which proteins are absolutely required for the formation of focal adhesions is still under investigation, and the order with which these proteins bind integrins, actin, or each other is only partly understood. In addition, changes in cell shape and movement may require the transfer of mechanical forces between the cytoskeleton and ECM as well as changes in cytoskeletal organization [4–6]. The focal adhesion complex is a critical point for the regulation of actin organization [1] as well as mechanical signal transfer [7]. Recently, Crowley and Horwitz [8] have shown tyrosine phosphorylation to play a role in the signal transduction, the actin-based tension of focal contacts, and the release of cellular adhesions.

We have been studying a mutant F9 embryonic carcinoma cell line (called 5.51) that adheres poorly to substrates and does not differentiate into a polarized epithelium [9, 10]. The protein vinculin is not detected in 5.51 cells. Vinculin is a 117-kDa protein that localizes at focal contacts and intercellular adherens junctions [2, 11]. In both types of contacts, vinculin is thought to form a complex with a number of other components that serve to anchor actin filaments to the membrane. In focal adhesions, vinculin binds to talin [12], α -actinin [13], paxillin [14], actin [15], and forms homodimers [16]. The binding of vinculin to talin and actin is regulated by polyphosphoinositides [17] and inhibited by acidic phospholipids [18]. We have demonstrated the importance of vinculin in the defect in adhesion in 5.51 cells correcting the mutant phenotype by transfect-

tion of a cloned copy of the vinculin gene [19]. Varnum-Finney and Reichardt [20] came to similar conclusions using the neuronal cell line PC12 transfected with vectors expressing antisense vinculin RNA to reduce vinculin protein. They found that in vinculin-deficient PC12 cells growth cones advanced more slowly and filopodia and lamellipodia were less stable than control cells. Increasing vinculin expression in 3T3 cells also increased formation of focal contacts and stress fibers, enhanced cell spreading, and reduced cell motility [21]. In contrast, reduction of vinculin protein with an antisense vinculin RNA in 3T3 cells, and homologous recombination in F9 cells, resulted in poor spreading and increased motility [22–24]. These results raise the possibility that the absence of vinculin in 5.51 cells may decrease cell adhesion by inhibiting focal adhesion assembly and preventing actin polymerization, whereas overexpression of vinculin may restore adhesion and spreading by promoting recruitment of cytoskeletal proteins to the focal adhesion complex at the site of integrin binding. Alternatively, the presence of vinculin could promote cell spreading by providing a path for transfer of mechanical stresses that can drive cytoskeletal remodeling directly [4, 7, 25].

In this study, we attempted to discriminate between these different mechanisms by measuring the effects of loss or replacement of vinculin on transmembrane mechanical force transfer across integrins and alterations in F-actin in 5.51 cells. We present data showing that vinculin is important for the linkage of integrins to the cytoskeleton. We hypothesize and demonstrate that the ability of cells to extend lamellipodia and spread correlates directly with the efficiency of mechanical coupling via vinculin, rather than with a change in net actin polymerization or cross-linking.

MATERIALS AND METHODS

Cell culture. The wild-type and vinculin-transfected F9 cell lines were maintained on 1% gelatin-coated charged plastic culture dishes in high-glucose (4.5 g/L) Dulbecco's modified Eagle's medium supplemented with 10% calf serum and 1% L-glutamine, penicillin, and streptomycin. The 5.51 cells were grown in suspension in the same medium.

Antibodies and fluorescent probes. A mouse monoclonal antibody to bovine mammary gland epithelium α -actinin (catalogue number A-5044) was purchased from Sigma Chemical Co. (St. Louis, MO). Mouse monoclonal antibodies to human smooth muscle vinculin (catalogue number MAB 1624) and chicken paxillin (catalogue number MAB3060) were purchased from Chemicon International (Temecula, CA). A rabbit polyclonal antibody to human platelet talin was the generous gift of Dr. Keith Burridge (University of North Carolina, Chapel Hill). The anti-actin mouse monoclonal antibody, C4, raised against chicken gizzard actin was a gift from Dr. James Lessard (Children's Hospital Foundation for Medical Research, Cincinnati, OH). Rhodamine-phalloidin was purchased from Molecular Probes (Eugene, OR).

Time-lapse video microscopy. F9 cell lines were plated on 25-mm circular No. 1 glass coverslips which had been coated with a combina-

tion of 5 $\mu\text{g}/\text{cm}^2$ human fibronectin (cat No. 40008) and 1 $\mu\text{g}/\text{cm}^2$ poly-D-lysine (cat No. 40210, both Collaborative Research, Waltham, MA). A combination of fibronectin and poly-D-lysine was necessary to attach the nonadherent 5.51 cells to coverslips for fluorescent staining procedures (see below). The coverslips were inserted into a Leiden coverslip chamber (Medical Systems Corp., Greenvale, NY) and examined in a Zeiss Axiovert inverted microscope, using a 100X Plan-Neofluar objective lens and Nomarski differential interference contrast (DIC) optics. A Zeiss environmental microscope chamber was used to maintain the cell cultures at 37°C and 5% CO₂. Video images obtained with a Hammamatsu C2400 Newvicon camera were recorded onto a Sony LVR 5000 analog laser disc recorder at 15-s intervals. Time-lapse recording (partitioning of the laser disc, time intervals and playback) was controlled with a Toshiba laptop PC (Model No. T1600) installed with Bio-Rad 4D software. Image-1 software (Universal Imaging Corp., West Chester, PA) was used to enhance fine details (sharpening and increasing contrast) and to digitize the images for quantitation.

Determination of cell spreading. F9 cell lines were cultured on glass coverslips coated with fibronectin and poly-D-lysine as described above. The cells were fixed at 5 and 45 min after plating, stained for F-actin with rhodamine-phalloidin, and confocal images of the ventral surface of the cell in contact with the substrate were collected. The edge of the cell was defined as the border of F-actin staining at the cell periphery. The projection area of the cells was then determined by planimetry of the digitized confocal images using Image-1 software. One hundred cells were measured for each cell type and time point. Also, to eliminate the effects of cell-cell contacts on cell spreading, only cells not touching each other were measured.

Determination of polymerized and cross-linked actin. The amount of F-actin in the F9 cell lines was determined fluorometrically using a procedure adapted from [26]. All procedures were done at room temperature. F9 cells were plated in 10-cm plastic culture dishes precoated with fibronectin and poly-D-lysine (see above) at a concentration of 5×10^6 cells/dish. Six dishes were used for each cell line. Four hours after plating the dishes were rinsed twice with PBS to remove nonadherent cells and fixed for 15 min in 4% paraformaldehyde and 0.1% Triton X-100 in a buffer containing 60 mM Pipes, 25 mM HEPES, 10 mM EGTA, 1 mM MgCl₂ (pH 6.9). This buffer, called PHEM, was originally described by [27]. The plates were then washed twice in PHEM containing 0.1% saponin (saponin-PHEM) and stained for 1 h in rhodamine-phalloidin (0.5 μM in saponin-PHEM, 2 ml/dish). Following incubation, the cells were washed three times in saponin-PHEM and destained with absolute methanol (3 ml/dish). The amount of rhodamine-phalloidin was determined by measuring the fluorescence of the methanol in a SLM spectrofluorimeter (excitation at 550 nm; emission at 580 nm). The relative F-actin content was calculated by dividing the fluorescence emission by the number of cells per dish. The number of cells per dish was determined by counting the number of cells in 10 microscope fields (for each dish) using a 20X objective and phase-contrast optics and extrapolating the area counted to the total area of the dish.

The content of cross-linked actin in the F9 cell lines was determined by measuring the amount of actin associated with the Triton-insoluble cytoskeleton. F9 cells were plated and grown as described for measuring the relative amount of F-actin. The plates were rinsed twice with PBS and extracted for 5 min with PHEM containing 1% Triton X-100 and the following protease inhibitors; 1 mM PMSF and 10 mg/ml each of benzamidine HCl, aprotinin, and leupeptin. Following extraction, the attached cellular components were scraped from the dish, and the mixture was centrifuged for 15 min at 14,000g to separate the Triton-soluble supernatant from the Triton-insoluble pellet fractions. For SDS-polyacrylamide electrophoresis the Triton-soluble supernatants were mixed with 1/10th volume sample buffer [consisting of 2% SDS, 20% glycerol, and 0.2 M dithiothreitol in 50 mM Tris-glycine buffer (pH 6.8)], and the Triton-insoluble pellets

were sonicated for 10 s in 20 vol of sample buffer. All samples were boiled for 5 min prior to electrophoresis on SDS–polyacrylamide gels.

Electrophoresis and immunoblotting. Triton-soluble and -insoluble samples of F9 cells were electrophoresed on 5–15% SDS–polyacrylamide minigels [28] and then electrophoretically transferred onto 0.45- μ m-pore-size nitrocellulose (NC) paper (Bio-Rad, Richmond, CA) for 2 h at 0.5 A in a transfer buffer consisting of 10 mM 3-(cyclohexylamino)-1-propanesulfonic acid (pH 11) and 10% methanol. After washing in Tris-buffered saline, pH 7.4 (TBS), with 0.1% Tween 20 (three times, 15 min each), nonspecific antibody binding was blocked by incubating the NC paper in a blocking solution consisting of 3% bovine serum albumin (BSA) and 2% nonfat dry milk in TBS for 2 h at 37°C. The NC paper was incubated in antibodies (in blocking solution containing 0.2% NP-40) overnight at 4°C and washed three times (15 min each) in TBS with 0.1% NP-40. After the NC paper was incubated again in blocking solution for 1 h at 37°C bound antibodies were detected with a chemiluminescence detection system (ECL System, Amersham Corp.). To compare the relative amounts of actin and focal adhesion proteins in the Triton-soluble and -insoluble fractions, immunoblots were scanned with a Zeineh laser densitometer (Biomedical Instruments, Inc., Fullerton, CA) and the relative peak areas quantified on a PC using a computer graphics program. Linearity was established by varying the amount of sample and/or the length of autoradiographic exposure.

Measurement of mechanical stiffness. Using a procedure described by Wang *et al.* [7], F9 cells were plated (3×10^4 cells per well) on fibronectin- and poly-D-lysine-coated plastic wells (96-well Removawells, Immunolon, IL) and cultured for 12 h before addition of 6.0- μ m spherical ferromagnetic beads that were precoated with a synthetic RGD-containing peptide (Peptide 2000, Telios Pharmaceuticals, La Jolla, CA), which is a specific ligand for integrin receptors. After 10 min, unbound beads were washed away with DMEM containing 1% BSA and the wells were placed into the magnetic twisting device and maintained at 37°C. Controlled mechanical stresses were applied directly to cell surface integrins by mechanically twisting these surface-bound RGD-coated microbeads, as previously described [25]. Mechanical stiffness of the focal adhesion and internal cytoskeleton (i.e., its ability to resist mechanical deformation) was measured by quantitating angular strain after applying a twisting magnetic field of 13.3 Gauss (i.e., a stress of 40 dyn/cm²) to the attached RGD magnetic beads 20 s after they were initially magnetized by a 10- μ s 1000-Gauss magnetic pulse.

Confocal microscopy. F9 cell lines were cultured on glass coverslips coated with fibronectin and poly-D-lysine as described above. Twelve hours after plating, the cells were fixed in 4% paraformaldehyde for 15 min followed by three washes in phosphate-buffered saline (PBS, pH 7.4) and extracted for 2 min in 0.2% Triton X-100. All procedures were done at room temperature (~22°C). Following extraction, cells were washed for 10 min in PBS and then stained with rhodamine–phalloidin (diluted 1:100 in PBS). After staining, the coverslips were washed in PBS (three changes, 15 min each), and a drop of 1% *n*-propyl gallate (used to reduce photobleaching of fluorescence, Sigma Chemical Co.) in a 8:2 mixture of glycerol and PBS (pH 8.5) was added to each coverslip before sealing with nail polish. The samples were examined using a confocal imaging system [BioRad MRC 600 attached to a Zeiss Axiovert inverted microscope (Carl Zeiss Inc., Thornwood, NY)] with a 100X Zeiss Plan-Neofluar objective.

RESULTS

Cell spreading. Time-lapse video microscopy was used to examine and to compare the motile behavior of the wild-type and 5.51 cells (Fig. 1). Wild-type F9 cells adhered to fibronectin-coated surfaces by first sending

out long filopodia. This was soon followed by veil-like lamellipodia which increased the surface area of the cell's attachment to the substrate. After attachment, the cell periphery displayed retrograde waves of dorsal cytoplasm moving rearward toward the center of the cell. In contrast, 5.51 cells had numerous actively extending and retracting filopodia but no lamellipodia were observed [19, 29]. The motile behavior of 5.51 cells resembled that of wild-type cells in the early stages of attachment (compare Figs. 1F and 1A).

The time course and extent of spreading of the F9 cell lines were measured (Table 1). Five minutes after plating, the wild-type and 5.51 cells had the same projected cell area (mean value of 270 mm²). Over the next 45 min, the area of the wild-type cells more than doubled (to 650 mm²), while the size of 5.51 cells remained unchanged. These data were consistent with the Nomarski DIC images which showed that 5.51 cells did not spread on the substrate and remained rounded (see Fig. 1). In contrast, the projected areas of the vinculin-transfected 5.51 cells (Vin3 and Vin4) almost doubled from 5 to 45 min.

F-actin content. Rhodamine–phalloidin binding assays were carried out to determine the amount of polymerized (F-) and cross-linked actin in the different F9 cell lines. The 5.51 cells, 5.51Vin3, and 5.51Vin4 all contained between 80 and 95% of the amount of F-actin present in wild-type cells (Fig. 2). Thus, there was no correlation between the absence or presence of vinculin and the total amount of F-actin in 5.51 cells. To determine the amount of cross-linked actin in the F9 cell lines, detergent (Triton X-100)-soluble and -insoluble fractions were electrophoretically separated in 5–15% SDS–polyacrylamide gels (Fig. 3A), and the amount of actin present in the extracts was determined by densitometry of Coomassie blue-stained gels and immunoblots stained with anti-actin antibodies (see Materials and Methods). The insoluble fraction contained the detergent-resistant cytoskeleton including cross-linked actin filaments. There was no detectable difference in the distribution of actin in the detergent-soluble and -insoluble fractions of wild-type F9, 5.51, 5.51Vin3, and 5.51Vin4 cells (Fig. 3B). In all the cell lines, the detergent-soluble fraction contained 30% actin and the -insoluble fraction contained 70% actin. This result suggests that the amount of cross-linked actin in F9 cells also is not affected by the lack of vinculin.

Distribution of focal adhesion complex proteins in F9 cell detergent extracts. To determine if the absence of vinculin affected the amount and distribution of focal adhesion proteins in the detergent-soluble and -insoluble fractions (i.e., association with the detergent-resistant cytoskeleton), immunoblots of F9 cell extracts were stained with antibodies to focal adhesion proteins (Figs. 3C–3F). Based on densitometry, 40% of the total

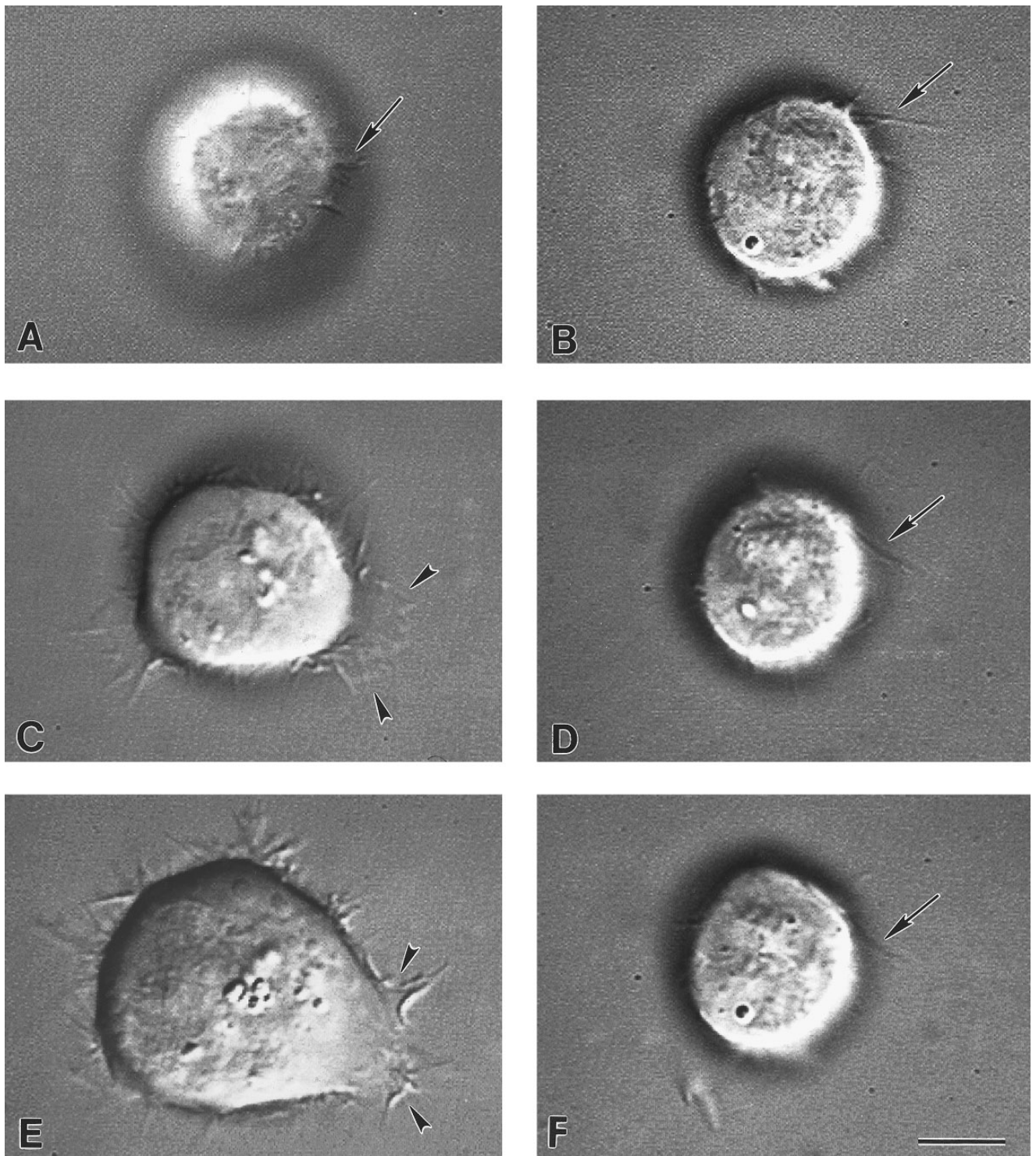


FIG. 1. Spreading of a wild-type F9 cell (A, C, E) and a vinculin-deficient 5.51 cell (B, D, F). Trypsinized cells were added to fibronectin-coated coverslips and examined from below with an inverted microscope using video-enhanced Nomarski DIC optics, and images were recorded onto a laser disk. Five minutes after addition to the coverslip (A), the wild-type cell was rounded and had filopodia that made contact with the substrate (arrow in A). At 10 (C) and 15 (E) min, the cell was flattened and lamellipodia (arrowheads) extended outward from the cell body. In contrast, the 5.51 cell remained rounded and only had extending and retracting filopodia (arrows in B, D, and F) when examined at the same time intervals as the wild-type cell. Bar in (F), 10 μ m.

TABLE 1

Time Course of Spreading of F9 Cell Lines

	5 min	45 min
Wild-type F9	273 (± 25 ; 100)	592 (± 46 ; 100)
5.51	250 (± 32 ; 100)	286 (± 26 ; 100)
5.51Vin3	364 (± 56 ; 100)	605 (± 40 ; 100)
5.51Vin4	432 (± 45 ; 100)	665 (± 36 ; 100)

Note. The maximal projected area (μm^2) at the cell–substrate interface was measured for each cell type at 5 and 45 min after plating. At 45 min, the projected area of the wild-type cells increased twofold, whereas the 5.51 cells remained unchanged. In contrast, the projected area of the vinculin-transfected 5.51 Vin3 and Vin4 cells increased close to twofold 45 min after plating. The standard deviation and the number of measurements are given in parentheses.

vinculin was in the cytoskeleton fraction in wild-type F9 cells. Vinculin protein was not detected in extracts of 5.51 cells. In 5.51Vin3 cells, which express 20-fold more vinculin than wild-type cells [19], 20% of the vinculin was in the cytoskeleton fraction, whereas 50% of vinculin was in the cytoskeleton fraction of 5.51Vin4 cells which express moderate amounts of vinculin [19]. The amount of vinculin in the cytoskeleton fraction of 5.51Vin3 cells was equivalent to the amount of vinculin in the cytoskeleton in wild-type cells (Fig. 3B, compare lanes 1 and 3).

Staining of immunoblots of F9 cell detergent extracts with antibodies to α -actinin (Fig. 3D) showed that 70% of α -actinin was in the cytoskeleton fraction in wild-type cells. In contrast, in 5.51 cells, only 20% of α -actinin was in the cytoskeleton fraction. In 5.51Vin3 and 5.51Vin4 cells, the amounts of α -actinin in the cytoskeleton fractions were 50 and 70%, respectively. This was still greater than the 20% α -actinin present in the cytoskeletal fraction of 5.51 cells. These data suggest that the association of α -actinin with the cytoskeleton is affected by the amount of vinculin in the F9 cells. Since α -actinin organizes actin filaments into bundles and associates with stress fibers, the smaller proportion of α -actinin in the cytoskeleton fraction of 5.51 cells may be due to the absence of stress fibers in these cells [19, 29].

In immunoblots of detergent-extracted F9 cells stained with antibodies to paxillin (Fig. 3E), 40% of the total paxillin was in the cytoskeleton fraction of wild-type cells. In 5.51 cells, 15% of paxillin was in the cytoskeleton fraction, while 30% of paxillin was present in the cytoskeleton of 5.51Vin3 and Vin4 cells. The smaller proportion of cytoskeletal paxillin in 5.51 cells may be due to the absence of vinculin which binds directly to paxillin [14] and thus links it to actin filaments. Conversely, transfected vinculin may bind paxillin and thereby retain it in the cytoskeleton fraction (Fig. 3B, lanes 3). The amount of talin in the cytoskele-

ton fractions was unaffected by the amount of vinculin present in the F9 cell variants (Fig. 3F).

Immunolocalization of focal adhesion complex proteins. The F9 cell lines were stained with antibodies to α -actinin, paxillin, and talin and the localization of these proteins was compared with the distribution of F-actin. In wild-type F9 cells, α -actinin was distributed at intervals along actin stress fibers and was concentrated in focal contacts (Fig. 4). In the vinculin-deficient 5.51 cells, α -actinin colocalized with F-actin in the cell cortex and in filopodia. In 5.51Vin3 and Vin4 cells, α -actinin was distributed along stress fibers in the same stippled staining pattern observed in the wild-type cells. Since the distribution of α -actinin in all the F9 cell lines was determined by the organization of F-actin, the interaction of α -actinin with F-actin did not appear to be affected by the loss of vinculin.

In the wild-type F9 cells, paxillin and talin were all concentrated in focal contacts at the ends of stress fibers (Figs. 5 and 6). In 5.51 cells, however, talin colocalized with F-actin in patches near the plasma membrane, and paxillin was diffusely distributed in the cytoplasm. Since paxillin is known to bind only to vinculin, the diffuse distribution of paxillin in 5.51 cells may be directly due to the absence of vinculin. The transfection of vinculin into 5.51 cells restored the localization of paxillin and talin to the pattern observed in wild-type F9 cells, i.e., at the ends of stress fibers (Figs. 5 and 6, panels E–H).

Mechanical coupling of integrins to the cytoskeleton. The efficiency of mechanical force transfer between integrins and the cytoskeleton in F9 cells was determined using a magnetic twisting cytometer. Controlled mechanical stresses were applied directly to cell surface

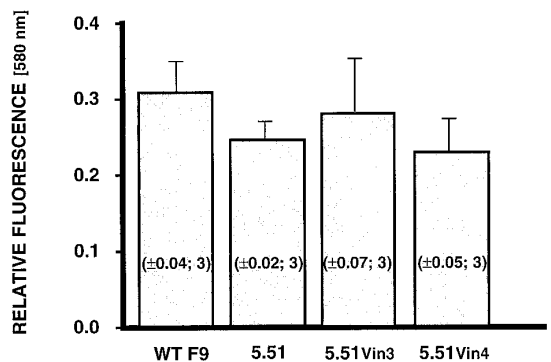


FIG. 2. F-actin content of F9 cell lines 4 h after plating on fibronectin- and poly-D-lysine-coated coverslips. The relative F-actin content was calculated by dividing the fluorescence emission of rhodamine-phalloidin determined at 580 nm by the number of cells per dish. The amount of F-actin in the vinculin-deficient (5.51) and vinculin-transfected (5.51Vin3 and Vin4) cells varied 80–95% in comparison to the wild-type F9 cells. The standard deviation and the number of measurements (for each sample) are given in parentheses.

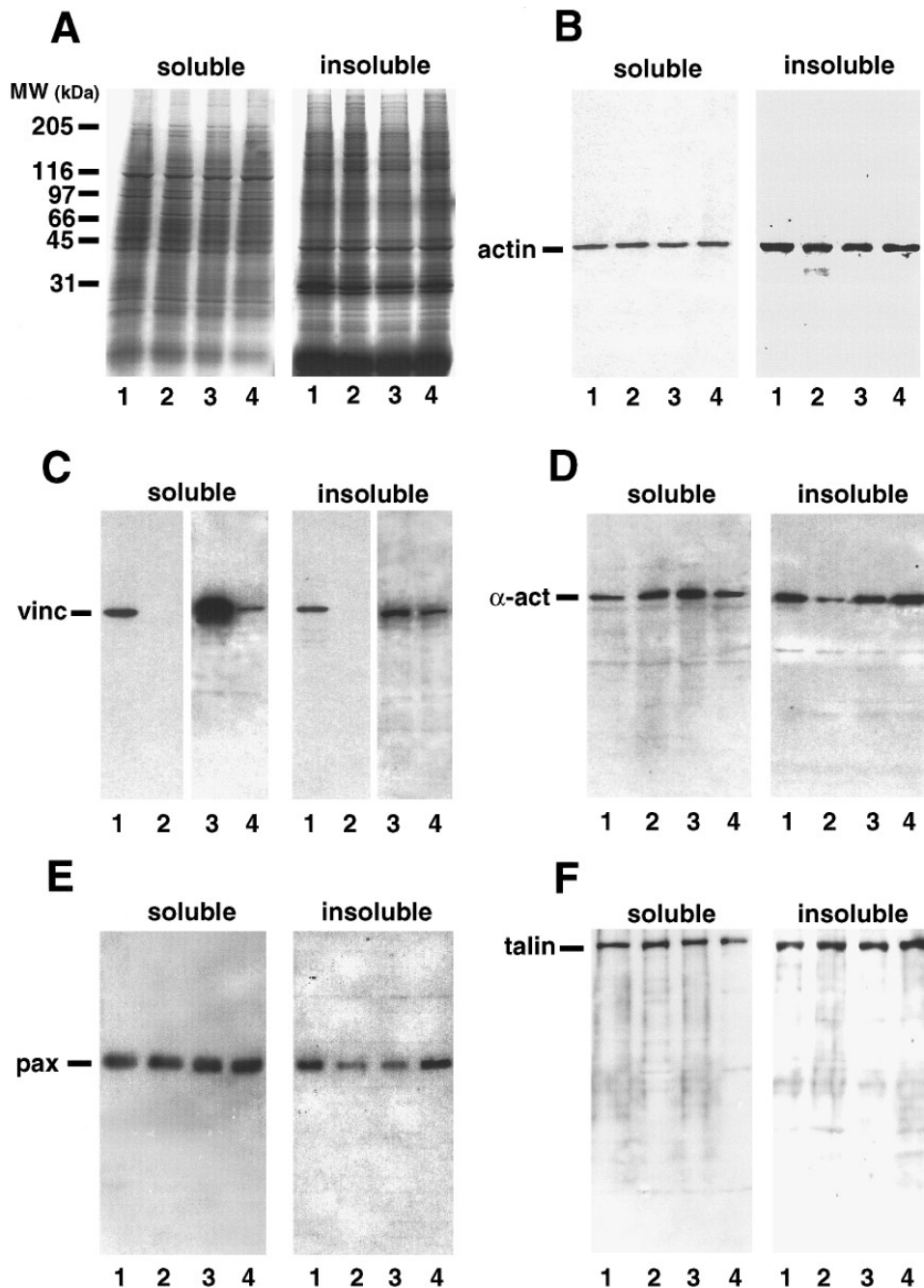


FIG. 3. (A) SDS-polyacrylamide gel electrophoresis of the detergent-soluble and -insoluble (cytoskeleton) fractions of wild-type F9 (lane 1), 5.51 (lane 2), 5.51Vin3 (lane 3), and 5.51Vin4 (lane 4) cells. Identical amounts of protein for each fraction and cell type were electrophoresed on 5–15% SDS-polyacrylamide gels and stained with Coomassie blue. (B–F) Distribution of actin and focal adhesion complex proteins in immunoblots of detergent-extracted F9 cells. Detergent-soluble and -insoluble fractions of wild-type F9 (lanes 1), 5.51 (lanes 2), 5.51Vin3 (lanes 3), and 5.51Vin4 (lanes 4) cells were electrophoresed on 5–15% SDS-polyacrylamide gels, transferred to nitrocellulose, and stained with antibodies to actin (B), vinculin (vinc, C), α -actinin (α -act, D), paxillin (pax, E), and talin (F).

integrins via bound RGD-coated magnetic microbeads and the cytoskeletal response was measured simultaneously using cell magnetometry [7]. Using this system, transmembrane integrin receptors that form focal adhesions and structurally couple to the internal cy-

toskeleton respond to stress application by getting stiffer and stiffer whereas transmembrane metabolic receptors show little resistance to stress. As shown in Fig. 7, the stiffness of the integrin-cytoskeletal linkages in 5.51 cells was reduced to >50% of that measured in

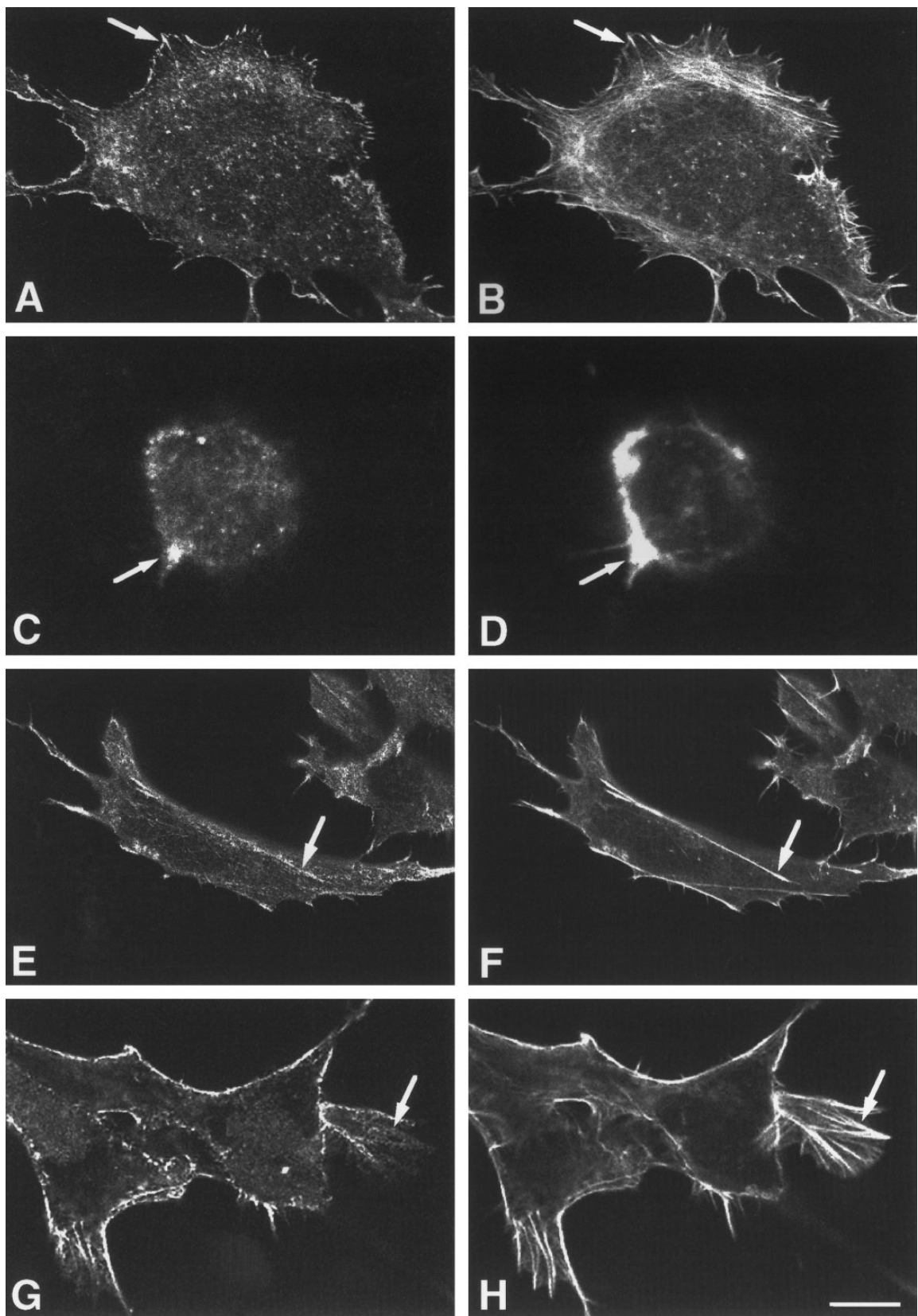


FIG. 4. Colocalization of α -actinin (A, C, E, and G) and F-actin (B, D, F, H) in wild-type F9 (A, B), 5.51 (C, D), and vinculin-transfected 5.51 [Vin3 (E, F) and Vin4 (G, H)] cells. Cells were stained with a mouse monoclonal antibody to human α -actinin and then with rhodamine-phalloidin. In the wild-type cells, α -actinin was associated with stress fibers in a stippled pattern (arrows in A and B). In the 5.51 cell, α -actinin was associated with F-actin in the cytoplasm and filopodia (arrows in C and D). In 5.51Vin3 and Vin4 cells, α -actinin was associated with the restored stress fibers (arrows in E–H). (G and H) Two 5.51Vin4 cells in contact. Bar (in H), 4 μ m for wild-type F9, 5.51Vin3, and Vin4 cells; 3 μ m for 5.51 cells.

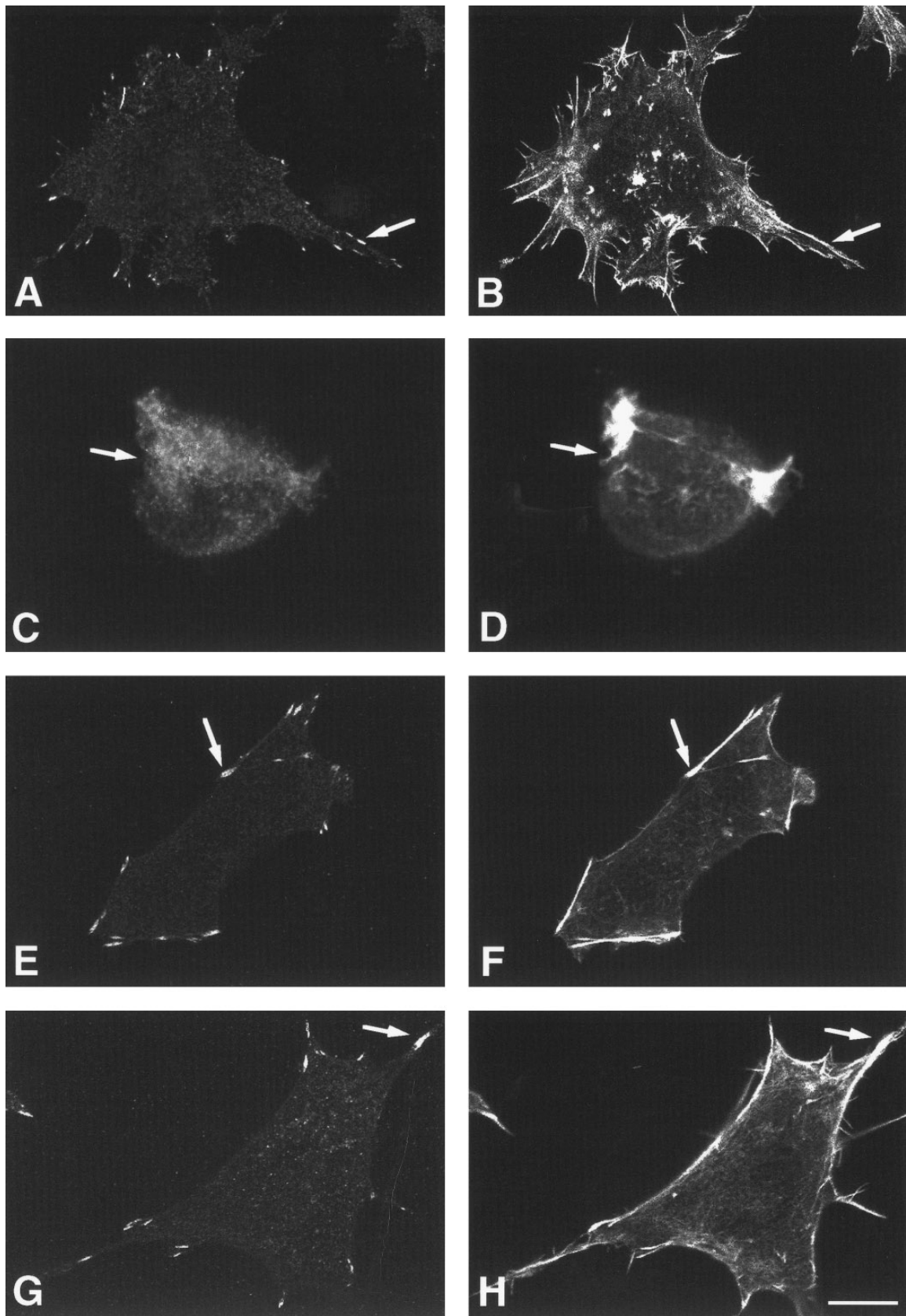


FIG. 5. Colocalization of paxillin (A, C, E, and G) and F-actin (B, D, F, H) in wild-type F9 (A, B), 5.51 (C, D), and vinculin-transfected 5.51 [Vin3 (E, F) and Vin4 (G, H)] cells. Cells were stained with a mouse monoclonal antibody to paxillin and then with rhodamine-phalloidin. In wild-type cells, paxillin was concentrated at the ends of stress fibers in focal contacts (arrows in A and B). In 5.51 cells, paxillin was diffusely distributed in the cytoplasm, including filopodia (arrows in C and D). In 5.51Vin3 and Vin4, paxillin was concentrated at the ends of stress fibers (arrows in E–H). Bar (in H), 4 μm for wild-type F9, 5.51Vin3 and Vin4 cells; 3 μm for 5.51 cells.

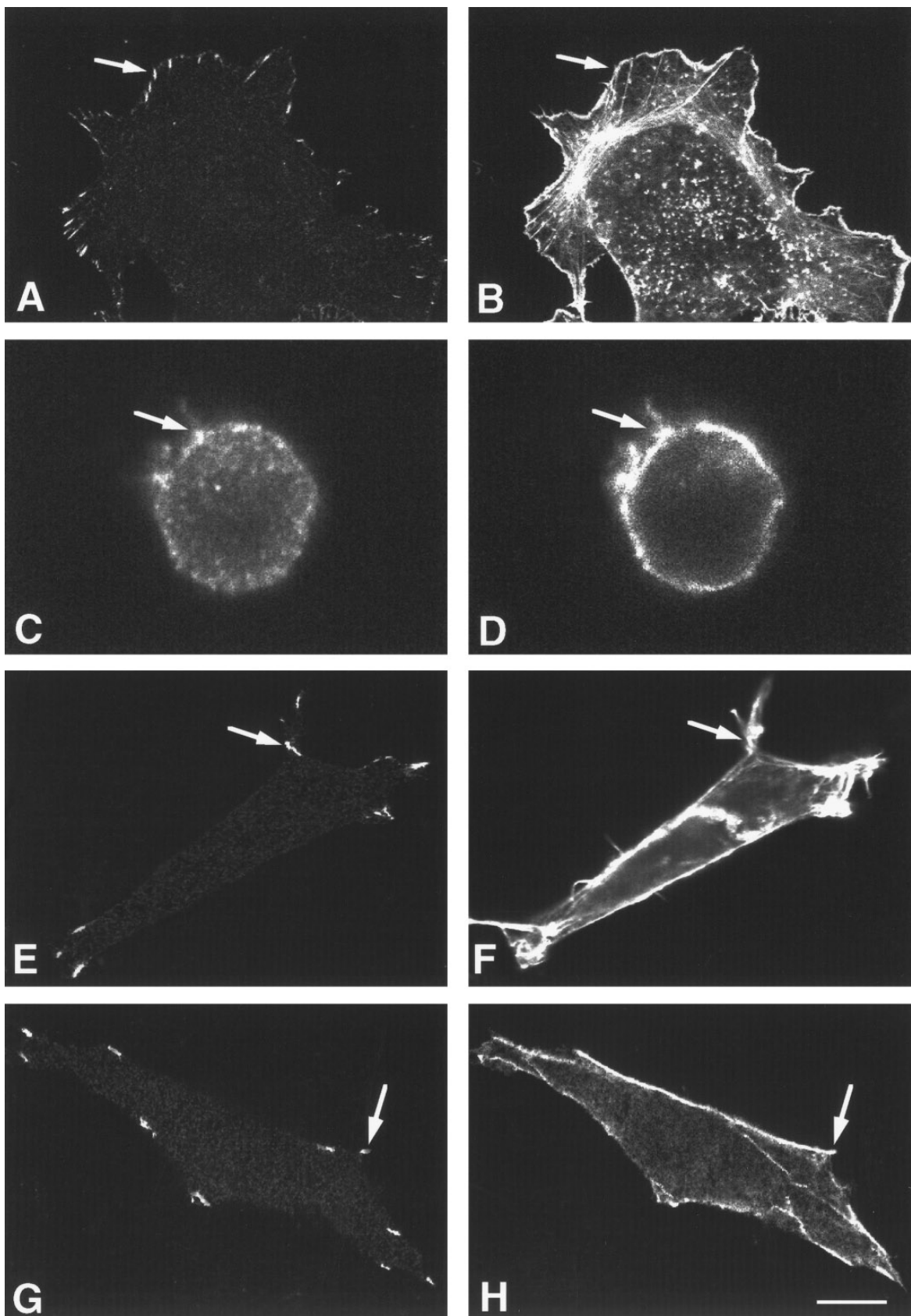


FIG. 6. Colocalization of talin (A, C, E, and G) and F-actin (B, D, F, H) in wild-type F9 (A, B), 5.51 (C, D), and vinculin-transfected 5.51 [Vin3 (E, F) and Vin4 (G, H)] cells. Cells were stained with a rabbit polyclonal antibody to talin and then with rhodamine-phalloidin. In wild-type cells, talin was concentrated at the ends of stress fibers in focal contacts (arrows in A and B). In 5.51 cells, talin was present in patches throughout the cell, including filopodia (arrows in C and D). (E and F) The localization of talin in focal contacts (arrows) was restored in 5.51Vin3 and Vin4 cells transfected with vinculin. Bar (in H), 4 μm for wild-type F9, 5.51Vin3, and Vin4 cells; 3 μm for 5.51 cells.

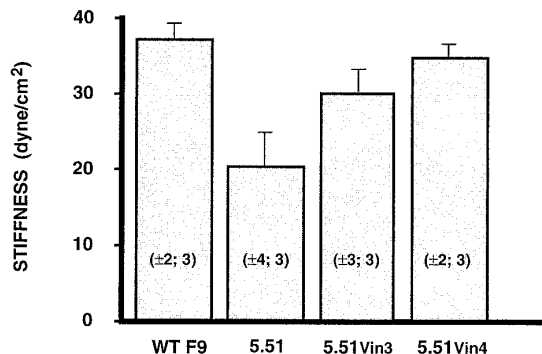


FIG. 7. Stiffness (calculated as the stress divided by the strain) of RGD-coated magnetic microbeads bound to the surface of wild-type F9, 5.51, and vinculin-transfected (5.51Vin3 and 5.51Vin4) cells. The standard deviation and the number of measurements (for each sample) are given in parentheses.

the wild-type cells (20 versus 37 dyn/cm²). Transfection of vinculin into 5.51 cells restored the mechanical linkage to the integrin-linked cytoskeleton (see Fig. 7). These results indicate that the focal adhesions that form in response to RGD-bead binding in 5.51 cells were less able to resist mechanical deformation and less effective at transmitting mechanical stress to the internal cytoskeleton. Confocal microscopy confirmed that less F-actin was associated with the RGD-beads in 5.51 cells than in wild-type cells (Fig. 8). The absence of an extensive F-actin network in this region may, in part, account for the decreased resistance to magnetic twisting exhibited by 5.51 cells.

DISCUSSION

To understand the role of vinculin in cell shape control, it is necessary to consider the biophysical basis of

adhesion and spreading. When an anchorage-dependent cell adheres to a rigid ECM substrate, forces due to local integrin binding begin to drive membrane flattening until balanced by the mechanical stiffness of the cortical membrane and associated cytoskeleton. Normal cells overcome these forces by clustering multiple integrins together with actin-associated molecules within localized focal adhesion complexes that, in turn, physically couple to the ends of actin microfilaments inside the cell. Formation of this molecular bridge results in outward transfer of cytoskeletal tension to the cell's ECM adhesions, resulting in what is known as a "strengthening response" [30]. If the ECM can resist these contractile forces (i.e., resist bending or compression), then the cell can extend outward and progressively change from a spherical to a more flattened or spread morphology. Our results show that loss of vinculin in 5.51 cells, disrupts focal adhesion complex formation, decreases the efficiency of transmembrane mechanical coupling, and prevents cell adhesion and spreading. More importantly, all of these deficiencies could be reversed by replacing vinculin through transfection in two different F9 cell lines. Thus, at least in 5.51 cells, vinculin appears to play a key role in shape control based on its ability to modulate focal adhesion structure and function.

Most past work on cell shape control focused on the mechanism by which motile cells extend small processes, such as filopodia and lamellipodia. Much less is known about how cells change from round to spread following adhesion or when they are nonmotile. However, all cell shape changes are mediated through cytoskeletal reorganization. For example, suspended cells contain a continuous microfilament lattice that is loosely packed and isotropic (nonoriented) when round and free of anchorage [27, 31, 32]. As cells attach and

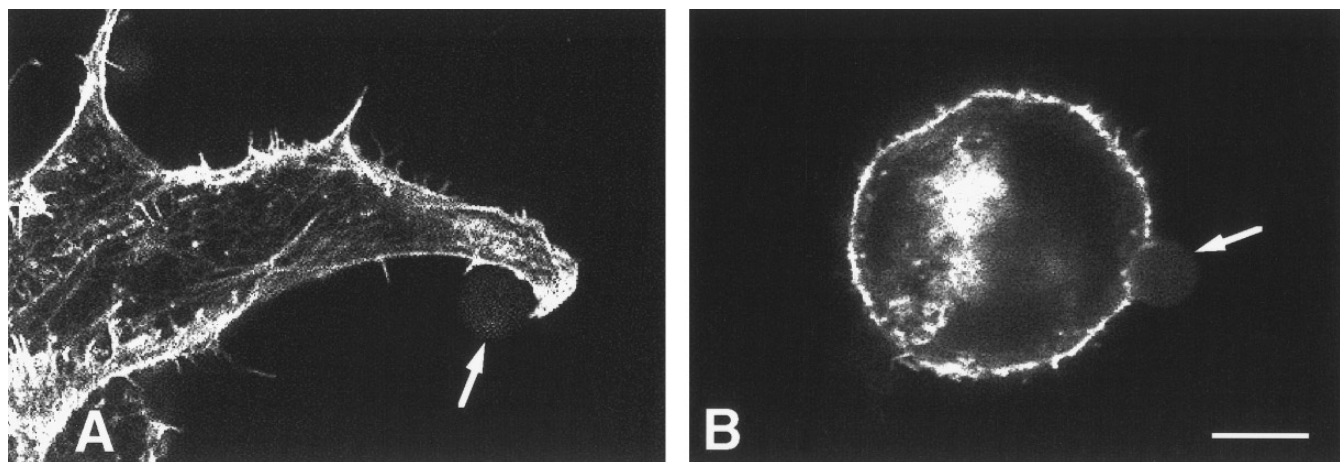


FIG. 8. Organization of F-actin in wild-type F9 (A) and 5.51 (B) cells that have bound RGD-coated magnetic microbeads (arrows). Increased cortical actin and a dense cytoplasmic actin network was observed at the site of RGD-bead binding in the wild-type F9, but not 5.51, cells. Bar (in B), 3 μ m.

spread on extracellular matrix, this loose network remodels locally between fixed focal adhesions and forms microfilament bundles that are known as “stress fibers.” Importantly, these changes in microfilament organization and cell shape proceed without altering total microfilament number [33] or the total amount of F-actin [6, 34]. In fact, one possibility is that these changes in cytoskeletal organization result from “tension-molding” of the flexible microfilament networks when cells apply tension to ECM and thereby increase isometric tension in the cytoskeleton that stretches between isolated focal adhesions [4, 35, 36]. Our finding that transfection of vinculin into 5.51 cells promoted stress fiber formation and cell spreading by stabilizing focal adhesions and supporting transfer of mechanical stresses across the cell surface, rather than by altering the total amount of F-actin polymer or cross-linking, is consistent with this hypothesis. In fact, “stress fiber” formation can be artificially induced by applying mechanical tension to the cell surface both *in vitro* [37, 38] and *in vivo* [39].

Work on the cytoskeletal basis of cell motility has revealed that formation of both filopodia and lamellipodia involves changes in microfilament assembly. The stiff actin bundles that form the central cores of filopodia and extend from the central microfilament lattice [40, 41] and push the cortical membrane outward are a result of actin polymerization, either alone or in combination with osmotic forces [42–45]. Vinculin apparently is not required for this form of actin assembly given that 5.51 cells continued to extend filopodia, even when round. In contrast, lamellipodial extension was only observed in cells that contained vinculin. Some models of lamellipodial formation similarly depend on actin polymerization, alone or in combination with osmotic forces [42–45]. Others are based on myosin-dependent movements of actin filaments at the leading edge [46, 47]. The vinculin-deficient 5.51 cells contained normal amounts of talin and α -actinin, two focal adhesion proteins capable of binding actin [48, 49], but their presence alone was not sufficient to induce formation of lamellipodia or stress fibers. Actin polymerization per se clearly was not inhibited since filopodia extended normally in 5.51 cells and there was no significant difference in the total amount of F-actin polymer in the four different F9 cell lines. There also was no difference in total actin cross-linking.

One interpretation of these results is that talin supports linear membrane extension (i.e., filopodia) driven by actin polymerization, in the absence of vinculin. While talin self-associates to form dimers, vinculin forms multimers [16, 50]. Furthermore, talin dimers may themselves be linked by vinculin [51]. In addition, vinculin binds to α -actinin, an actin cross-linking protein, while talin does not. In this manner, vinculin may support the broader, more stable cytoplasmic exten-

sions of lamellipodia while in its absence, only filopodia would form. Another possibility is that vinculin promotes lamellipodia extension and cell spreading indirectly by stabilizing focal adhesion structure (e.g., stiffness), as demonstrated in the magnetic bead twisting studies. This, in turn, would allow cells to exert cytoskeletal tension on the extracellular matrix, increase internal isometric tension within the whole cytoskeleton and, hence, to drive local cytoskeletal remodeling events in the apex of the cell as well as at the cell base. For example, structural modeling studies show that increased isometric tension in the cytoskeleton can explain how triangulated nets of microfilaments form in apical regions of spreading cells as well as basal stress fibers, in the absence of net changes in actin polymerization or cross-linking [4, 5]. Importantly, vertices of triangulated actin nets (e.g., actin geodomes) appear to serve as preferred niduses for actin polymerization [40, 41]. Thus, failure to form well-developed focal adhesions in the vinculin-deficient cells could result in both decreased stiffening and incomplete tension molding of the actin cytoskeleton. This would suppress both lateral membrane extension and cell spreading.

Key to all of these processes is the clustering of integrins and the formation of a stable focal adhesion complex that can bear mechanical loads. The presence of focal adhesions, as monitored by interference reflection microscopy and staining for characteristic proteins (e.g., α -actinin, paxillin, and talin), coincided with the loss and reintroduction of vinculin in F9 cells [19, 29]. Furthermore, using atomic force microscopy and rheology, the 5.51 cells displayed marked differences in viscoelasticity [52]. Although the sequence of events leading to focal adhesion complex formation is not fully understood there is reason to believe that adhesion can be established by an alternative mechanism(s) involving α -actinin or talin, both of which can bind to actin and integrins [23, 24, 53, 54]. For example, talin and F-actin can accumulate before vinculin at the site where focal adhesions will eventually form in spreading fibroblasts [55, 56]. Talin also colocalizes with F-actin in patches near the plasma membrane in 5.51 cells. Our mechanical twisting data also show that F9 cells exhibit some mechanical coupling between integrins and the cytoskeleton. However, the presence of vinculin appears to be required for optimal mechanical stability of the focal adhesion complex, a structural feature that appears to be critical for cell adhesion and spreading as well as cytoskeletal reorganization.

Recently, a vinculin knockout was created by homologous recombination. These cells differ from the 5.51 cells in that adhesion is only slightly inhibited [23, 24]. It is possible that knocking out vinculin in these cells has produced some compensatory mechanism that is not found in 5.51 cells or there is some other caveat that remains to be determined. However, regardless of

the differences between these two models, the present results show that loss of vinculin produces a particular phenotype in 5.51 cells and that most—if not all—of this phenotype can be reversed by vinculin transfection. In summary, many models have been proposed to explain how cells change shape and move. However, all of these models require that the cell must adhere to an extracellular matrix substrate that can resist cell-generated forces in order to promote cytoskeletal rearrangements necessary for global cell shape changes and to propel the cell forward. Many molecules are known to localize to the site of integrin clustering within the focal adhesion complex; however, their structural functions remain unknown. The results of the present study show that vinculin controls adhesion, cytoskeletal remodeling, and cell spreading by mechanically stabilizing the molecular bridge between actin and integrins that forms the core of the focal adhesion and thereby, enhancing its ability to both transmit and resist cytoskeletal tension.

We thank Dr. Eileen Adamson for providing the F9 cell lines and helpful comments. This work was supported by the American Cancer Society, NASA, Deutsche Forschungsgemeinschaft, and NATO. Dr. Ingber is a recipient of a Faculty Research Award from American Cancer Society.

REFERENCES

- Luna, E., and Hitt, A. L. (1992) *Science* **258**, 955–963.
- Burridge, K., Fath, K., Kelly, T., Nuckolls, G., and Turner, C. (1988) *Annu. Rev. Cell Biol.* **4**, 487–525.
- Jockusch, B. M., Bubeck, P., Giehl, K., Kroemker, M., Moschner, J., Rotkegel, M., Ruediger, M., Schiller, K., Stanke, G., and Winkler, J. (1995) *Annu. Rev. Cell Dev. Biol.* **11**, 379–416.
- Ingber, D. E. (1993) *J. Cell Sci.* **104**, 613–627.
- Ingber, D. E., Dike, L., Hansen, L., Karp, S., Liley, H., Maniotis, A., McNamee, H., Mooney, D., Plopper, G., Sims, J. *et al.* (1994) *Int. Rev. Cytol.* **150**, 173–224.
- Mooney, D. J., Langer, R., and Ingber, D. E. (1995) *J. Cell Sci.* **108**, 2311–2320.
- Wang, N., Butler, J. P., and Ingber, D. E. (1993) *Science* **260**, 1124–1127.
- Crowley, E., and Horwitz, A. F. (1995) *J. Cell Biol.* **131**, 525–537.
- Grover, A., Rosentraus, M. J., Serman, B., Snook, M. E., and Adamson, E. D. (1987) *Dev. Biol.* **120**, 1–11.
- Calogero, A., Samuels, M., Darland, T., Edwards, S. A., Kemler, R., and Adamson, E. D. (1991) *Dev. Biol.* **146**, 499–508.
- Jockusch, B. M., and Isenberg, G. (1981) *Proc. Natl. Acad. Sci. USA* **78**, 3005–3009.
- Burridge, K., and Mangeat, P. (1984) *Nature* **308**, 744–746.
- Wachsstock, D. H., Wilkins, J. A., and Lin, S. (1987) *Biochem. Biophys. Res. Commun.* **146**, 554–560.
- Turner, C. E., Glenney, J. R., Jr., and Burridge, K. (1990) *J. Cell Biol.* **111**, 1059–1068.
- Johnson, R. P., and Craig, S. W. (1994) *J. Biol. Chem.* **269**, 12611–12619.
- Johnson, R. P., and Craig, S. W. (1995) *Nature* **373**, 261–264.
- Gilmore, A. P., and Burridge, K. (1996) *Nature* **381**, 531–535.
- Weekes, J., Barry, S. T., and Critchley, D. R. (1996) *Biochem. J.* **314**, 827–832.
- Samuels, M., Ezzell, R. M., Cardozo, T. J., Critchley, D. R., Coll, J. L., and Adamson, E. D. (1993) *J. Cell Biol.* **121**, 909–921.
- Varnum-Finney, B., and Reichardt, L. F. (1994) *J. Cell Biol.* **127**, 1071–1084.
- Rodriguez Fernandez, J. L., Geiger, B., Salomon, D., and Ben-Ze'ev, A. (1992) *Cell Motil. Cytoskeleton* **22**, 127–134.
- Rodriguez Fernandez, J. L., Geiger, B., Salomon, D., Sabanay, I., Zoller, M., and Ben-Ze'ev, A. (1992) *J. Cell Biol.* **119**, 427–438.
- Volberg, T., Geiger, B., Kam, Z., Pankov, R., Simcha, I., Sabanay, H., Coll, L. J., Adamson, E. D., and Ben-Ze'ev, A. (1995) *J. Cell Sci.* **108**, 2253–2260.
- Coll, J. L., Ben-Ze'ev, A., Ezzell, R. M., Rodriguez Fernandez, J. L., Baribault, H., Oshima, R. G., and Adamson, E. D. (1995) *Proc. Natl. Acad. Sci. USA* **92**, 9161–9165.
- Wang, N., and Ingber, D. E. (1994) *Biophys. J.* **66**, 2181–2189.
- Condeelis, J., and Hall, A. L. (1991) *Methods Enzymol.* **196**, 486–496.
- Schliwa, M., van Blerkom, J., and Porter, K. (1981) *Proc. Natl. Acad. Sci. USA* **80**, 5417–5420.
- Matsudaira, P. T., and Burgess, D. R. (1978) *Anal. Biochem.* **87**, 386–396.
- Goldmann, W. H., Schindl, M., Cardozo, T. J., and Ezzell, R. M. (1995) *Exp. Cell Res.* **221**, 311–319.
- Lotz, M. M., Burdsal, C. A., Erickson, H. P., and McClay, D. R. (1989) *J. Cell Biol.* **109**, 1795–1805.
- Ben-Ze'ev, A., Duerr, A., Salomon, F., and Penman, S. (1979) *Cell* **17**, 859–865.
- Heuser, J., and Kirschner, M. (1980) *J. Cell Biol.* **86**, 212–234.
- Revel, J. P., Hoch, P., and Ho, D. (1974) *Exp. Cell Res.* **84**, 207–218.
- Bereiter-Hahn, J., Luck, M., Miebach, T., Stelzer, H. K., and Voth, M. (1990) *J. Cell Sci.* **96**, 171–188.
- Bereiter-Hahn, J. (1987) in *Cytomechanics: The Mechanical Basis of Cell Form and Structure* (Bereiter-Hahn, J., Anderson, O. R., and Reif, W. E., Eds.), pp. 3–30, Springer-Verlag, Berlin.
- Opas, M. (1987) in *Cytomechanics: The Mechanical Basis of Cell Form and Structure* (Bereiter-Hahn, J., Anderson, O. R., and Reif, W. E., Eds.), pp. 273–286, Springer-Verlag, Berlin.
- Franke, R. P., Grafe, M., Schnittler, H., Seiffge, D., Mittermayer, C., and Drenckhahn, D. (1984) *Nature* **307**, 648–649.
- Kolega, J. (1986) *J. Cell Biol.* **102**, 1400–1411.
- Wong, A. J., Pollard, T. D., and Herman, I. M. (1983) *Science* **219**, 867–869.
- Lazarides, E. (1976) *J. Cell Biol.* **68**, 202–219.
- Osborn, M., Born, T., Koitsch, H. J., and Weber, K. (1978) *Cell* **14**, 477–488.
- Wang, J. L. (1986) *J. Cell Biol.* **101**, 597–602.
- Forscher, P., and Smith, S. (1988) *J. Cell Biol.* **107**, 1505–1516.
- Oster, G. F., and Perelson, A. A. (1987) *J. Cell Sci. Suppl.* **8**, 35–54.
- Small, J. (1989) *Curr. Opin. Cell Biol.* **1**, 75–79.
- Sheetz, M. P., Wayne, D. B., and Pearlman, A. L. (1992) *Cell Motil. Cytoskeleton* **22**, 160–169.
- Heath, J. P., and Holifield, B. F. (1991) *Cell Motil. Cytoskeleton* **18**, 245–257.

48. Goldmann, W. H., and Isenberg, G. (1991) *Biochem. Biophys. Res. Commun.* **178**, 718–723.
49. Muguruma, M., Matsumura, S., and Fukazawa, T. (1992) *J. Biol. Chem.* **267**, 5621–5624.
50. Goldmann, W. H., Bremer, A., Haener, M., Aebi, U., and Isenberg, G. (1994) *J. Struct. Biol.* **112**, 3–10.
51. Gilmore, A. P., Wood, C., Ohanian, V., Jackson, P., Patel, B., Rees, D. J. G., Hynes, R. O., and Critchley, D. R. (1993) *J. Cell Biol.* **122**, 337–347.
52. Goldmann, W. H., and Ezzell, R. M. (1996) *Exp. Cell Res.* **226**, 234–237.
53. Goldmann, W. H., Ezzell, R. M., Adamson, E. D., Niggli, V., and Isenberg, G. (1996) *J. Muscle Res. Cell Motil.* **17**, 1–5.
54. Jockusch, B. M., and Ruediger, M. (1996) *Trends Cell Biol.* **6**, 311–315.
55. DePasquale, J. A., and Izzard, C. S. (1987) *J. Cell Biol.* **105**, 2803–2809.
56. DePasquale, J. A., and Izzard, C. S. (1991) *J. Cell Biol.* **113**, 1351–1359.

Received August 21, 1996

Revised version received November 15, 1996